ELSEVIER

Effect of DNA damage on PCR amplification efficiency with the relative threshold cycle method

Jan A. Sikorsky[a], Donald A. Primerano[a,*], Terry W. Fenger[a], James Denvir[a,b]

[a] *Department of Microbiology, Immunology and Molecular Genetics, Joan C. Edwards School of Medicine,*
Marshall University, Huntington, WV 25704, USA
[b] *Department of Mathematics, Marshall University, Huntington, WV 25701, USA*

Abstract

Polymerase stop assays used to quantify DNA damage assume that single lesions are sufficient to block polymerase progression. To test the effect of specific lesions on PCR amplification efficiency, we amplified synthetic 90 base oligonucleotides containing normal or modified DNA bases using real-time PCR and determined the relative threshold cycle amplification efficiency of each template. We found that while the amplification efficiencies of templates containing a single 8-oxo-7,8-dihydro-2′-deoxyguanosine (8-oxodG) were not significantly perturbed, the presence of a single 8-oxo-7,8-dihydro-2′-deoxyadenosine, abasic site, or a *cis–syn* thymidine dimer dramatically reduced amplification efficiency. In addition, while templates containing two 8-oxodGs separated by 13 bases amplified as well as the unmodified template, the presence of two tandem 8-oxodGs substantially hindered amplification. From these findings, we conclude that the reduction in polymerase progression is dependent on the type of damage and the relative position of lesions within the template.
© 2004 Elsevier Inc. All rights reserved.

Keywords: DNA damage; Base modification; *Taq* polymerase; Real-time PCR; Amplification efficiency

DNA in living cells can be damaged by chemical and physical processes. For example, reactive oxygen species can react with 2′-deoxyguanosine to form 8-oxo-7,8-dihydro-2′-deoxyguanosine (8-oxodG) or with 2′-deoxyadenosine to form 8-oxo-7,8-dihydro-2′-deoxyadenosine (8-oxodA) [1–4]. These and other modified bases have altered base pairing properties which can lead to substitution mutations. Inherited defects in DNA repair pathways confer susceptibility to certain cancers and developmental disorders. These observations suggest that DNA damage is a preliminary step in carcinogenesis and may play a role in the aging process [5–7]. Assays for DNA damage are therefore needed for experimental monitoring of DNA repair pathways and clinical diagnosis of DNA repair defects [8].

Several assays have been developed to determine the extent of DNA damage and subsequent repair in living cells [8–15]. Detection by Southern analysis involves treatment of damaged DNA with lesion-specific endonucleases followed by hybridization of filter-bound restriction fragments to a gene-specific probe. Lesion-specific digestion reduces the signal intensity of the target gene and the frequency of lesions is proportional to the decrease in probe hybridization [9,10]. The requirement for relatively large amounts of DNA in this method led to the development of quantitative polymerase chain reaction (QPCR) methods [8,11–15]. These methods are based on the blocking of thermostable DNA polymerase progression by lesions in the DNA template which results in a decrease in the overall rate of PCR product formation [8,13–15]. Under the assumption that a single lesion is sufficient to block polymerase progression, the QPCR method effectively measures the fraction

---

* Corresponding author. Fax: +1 304 696 7354.
E-mail address: primeran@marshall.edu (D.A. Primerano).

of undamaged templates. DNA damage results in a reduction in template amplification and can be expressed as lesions per kilobase. Using this method, differences in the rates of DNA repair between mitochondrial (mtDNA) and nuclear DNA have been documented [13].

The polymerase chain reaction measured in real time is becoming the standard method for quantifying DNA and RNA [16,17]. Several mathematical methods are available for determining the input template copy number from real-time PCR data. Threshold cycle (C_T) methods determine input template amounts by comparing the C_T value from an unknown template to C_T values from templates of known copy number [18,19]. In the standard curve method, C_T is plotted against the logarithm of copy number for a series of known input templates and the copy number of the unknown template is determined by linear regression [18]. When using a standard curve method, either relative or absolute quantification can be achieved [18]. The comparative threshold method expresses relative changes in gene expression with normalization to a reference (housekeeping) gene using the $2^{-\Delta\Delta C_T}$ formula [19]. The method rests on the assumptions that the amplification efficiencies of the target and reference genes are approximately equal and that the amplification efficiencies of both genes in exponential phase are close to one [19]. In an alternative method developed by Liu and Saint [20], amplification efficiencies derived from kinetic curves are used to determine relative transcript abundance. This method does not require equivalent amplification efficiencies and obviates the need for standard curve construction. More recently, these workers observed that amplification efficiencies change dynamically during simulated PCRs and validated a mathematical method in which input template amounts are determined from amplification curve parameters [21].

Although the effect of base modifications on *Escherichia coli* DNA polymerase progression has been documented by several groups [3,22–26], their effects on *Taq* polymerase progression and PCR amplification efficiency have not been well characterized [27]. To study the influence of defined lesions on PCR amplification efficiency, we synthesized a series of 90 base oligonucleotides containing 8-oxodG, 8-oxodA, an abasic site, or a *cis–syn* cyclobutane thymidine dimer (TT dimer) and amplified them using real-time PCR. We developed a new method for determining the amplification efficiency of *Taq* polymerase based on the comparative threshold method of Livak and Schmittgen [19] and found that: (1) the amplification efficiencies of templates containing single 8-oxodA, abasic, or TT dimer base lesions were drastically reduced in comparison to unmodified templates, (2) the amplification efficiency of templates with a single 8-oxodG was equivalent to the unmodified template, and (3) the juxtaposition of two 8-oxodG bases dramatically reduced amplification rates.

Materials and methods

Preparation of oligonucleotide templates. Ninety base oligonucleotides were synthesized on an Applied Biosystems (ABI, Foster City, CA) Model 394 DNA Synthesizer in the Marshall University DNA Core Facility using low volume 200 nmol cycles with 30 s coupling time and standard phosphoramidite chemistry [28,29]. The sequence of the unmodified 90 base oligonucleotide was equivalent to a portion of the human mitochondrial Hypervariable Region One (Anderson sequence 15989–16078 [30]). 7,8-Dihydro-8-oxo-2′-deoxyguanosine, 7,8-dihydro-8-oxo-2′-deoxyadenosine, abasic site (tetrahydrofuran analogue), and *cis–syn* thymidine dimer were introduced at specific positions as indicated in Table 1 using DNA damage base cyanoethyl phosphoramidites (Glen Research, Sterling, VA). Oligonucleotides were synthesized in the trityl-on mode and cleaved from the polystyrene resin with ammonium hydroxide; 8-oxodG containing templates were cleaved with ammonium hydroxide containing 0.25 M β-mercaptoethanol [24,31]. Oligonucleotides were purified using ABI OPC cartridges to remove failure sequences [32] and analyzed on Agilent BioAnalyzer RNA 6000 Nanochips (Agilent Technologies, Palo Alto, CA). All templates had a single major band at the expected size. Oligonucleotide templates were quantified by measuring optical density at 260 nm, evaporated to dryness, and stored at −80 °C. Oligonucleotide extinction coefficients were obtained using Oligo Primer Analysis Software v5.0 (Molecular Biology Insights, Cascade, CO). One hundred micromolar stock solutions of each 90-mer were prepared in low TE buffer (10 mM Tris, pH 8.0; 0.1 mM EDTA) and maintained at −20 °C to prevent template degradation.

Template amplification and real-time PCR. PCR primers were designed to amplify either the full-length 90-mer oligonucleotide or a 45 base region with no base modifications [the internal control region (ICR)] with ABI Primer Express Software v2.0. Our standard 25 μl PCR contained 12.5 μl ABI 2× SYBR Green PCR Master Mix, 9.5 μl of sterile deionized H_2O, 1 μl of oligonucleotide template, 1 μl of 10 μM forward PCR primer (5′-CCC AAA GCT AAG ATT-3′), and either 1 μl of 10 μM reverse PCR primer (5′-TTG ATG GGT GAG TCA-3′) for full template amplification or 1 μl of 10 μM internal control primer (5′-CAT GAA AGA ACA GAG-3′) for ICR amplification. A master mix without template was prepared based on the total number of reactions. Oligonucleotide templates ranging from 1 amole to 100 fmole were then added to complete the reaction. Amplifications were performed in 96-well plates and capped with optical grade ABI PCR strip caps. Templates were amplified under the following conditions: 50 °C for 2 min, 95 °C for 10 min, and then 40 cycles of 95 °C for 20 s, 54 °C for 30 s, and 60 °C for 1 min. PCR amplification and detection was carried out in an ABI Model 7000 Sequence Detection System (SDS) according to guidelines provided [18]. C_T and delta Rn values were exported from SDS data files in comma delimited (.csv) format. Microsoft Excel software was used to open .csv files and calculate RTC efficiencies.

Derivation of the relative threshold cycle method. We developed a method to estimate amplification efficiency (E) of modified templates based on the observed threshold cycle (C_T) for the full-length and ICR PCR products. Since the input template amounts in these two PCRs were equal, any increase in C_T must result from a decrease in amplification efficiency. For unmodified templates (e.g., the ICR), if amplification is 100% efficient, the exponential formation of PCR product is:

$$x_n = 2^n x_0, \tag{1}$$

where (x_n) is the total fluorescence at cycle number (n) and (x_0) is the input template fluorescence at $n = 0$ [18,33]. During amplification of the full-length modified oligonucleotide, unmodified products were formed which then served as templates in subsequent cycles. During the exponential phase of these reactions, the amount of unmodified product (y_n) at cycle number n is:

Table 1
90-mer oligonucleotides used as templates for the PCR

Template[a]	Oligonucleotide sequence
Oxo CONTROL	5'-CCCAAAGCTAAGAGATTCTAATTTAAACTATTCTCTGTTCTTTCATGGGGAAGCAGATTTGGGTACCACCCAAGTATTGACTCACCCATCAA-3'
OxodG1 (48)	5'-CCCAAAGCTAAGAGATTCTAATTTAAACTATTCTCTGTTCTTTCATGGXAAGCAGATTTGGGTACCACCCAAGTATTGACTCACCCATCAA-3'
OxndG2A (48,61)	5'-CCCAAAGCTAAGAGATTCTAATTTAAACTATTCTCTGTTCTTTCATGGXAAGCAGATTTGGXTACCACCCAAGTATTGACTCACCCATCAA-3'
OxodG2T (47–48)	5'-CCCAAAGCTAAGAGATTCTAATTTAAACTATTCTCTGTTCTTTCATGGXXAAGCAGATTTGGGTACCACCCAAGTATTGACTCACCCATCAA-3'
OxodA1 (49)	5'-CCCAAAGCTAAGAGATTCTAATTTAAACTATTCTCTGTTCTTTCATGGGYAGCAGATTTGGGTACCACCCAAGTATTGACTCACCCATCAA-3'
Abasic (49)	5'-CCCAAAGCTAAGAGATTCTAATTTAAACTATTCTCTGTTCTTTCATGGGZAGCAGATTTGGGTACCACCCAAGTATTGACTCACCCATCAA-3'
Dimer CONTROL	5'-CCCAAAGCTAAGAGATTCTAATTTAAACTATTCTCTGTTCTTTCATGGGTTGCAGATTTGCAGATTTGCAGATTTGACTCACCCATCAA-3'
TTdimer (49–50)	5'-CCCAAAGCTAAGAGATTCTAATTTAAACTATTCTCTGTTCTTTCATGGGDDGCAGATTTGGTTACCACCCAAGTATTGACTCACCCATCAA-3'

[a] The position of modification relative to the 5' terminus of the oligonucleotide is indicated in parenthesis. X, Y, Z, and DD represent the insertion sites of 8-oxodG, 8-oxodA, Abasic, and cis–syn TT dimer modifications into the oligonucleotide. The dotted arrow, the solid arrow, and the dashed arrow indicate the binding sites of the forward, full-length amplicon reverse, and internal control region reverse primers, respectively.

$$y_n = 2y_{(n-1)} + EM, \qquad (2)$$

where (E) is the amplification efficiency of 8-oxodG templates and (M) is the fluorescence of modified templates. Prior to any amplification there was no unmodified template present in reactions using modified oligonucleotide as input template. With $y_0 = 0$ Eq. (2) becomes:

$$y_n = (2^n - 1)EM \qquad (3)$$

and the total PCR product (z_n) at cycle n is given by:

$$z_n = ((2^n - 1)E + 1)M. \qquad (4)$$

In order to determine threshold cycle for the ICR and full-length PCRs, we chose a threshold fluorescence (T), fixed for all reactions, which was sufficiently larger than the background fluorescence but small enough that the reaction was still in the exponential phase. The cycles at which the ICR and full-length PCRs reach the threshold level are designated (C_{TU}) and (C_{TM}). By substitution into Eqs. (1) and (4), we can derive equations that relate threshold fluorescence to cycle number for the ICR:

$$T = 2^{C_{TU}} x_0 \qquad (5)$$

and for the full-length PCR

$$T = ((2^{C_{TM}} - 1)E + 1)M. \qquad (6)$$

If $M = x_0$ for a given template, we can equate Eqs. (5) and (6), and solve for E:

$$E = (2^{C_{TU}} - 1)/(2^{C_{TM}} - 1). \qquad (7)$$

This equation can be approximated to produce the simpler equation:

$$E \cong 2^{C_{TU} - C_{TM}} \qquad (8)$$

which represents the relative threshold cycle (RTC) amplification efficiency. If $C_{TM} \geqslant C_{TU}$ and $C_{TM} > 11$ the error of this last approximation is less than 0.1%.

Results

Base modifications perturb amplification efficiency to different degrees

In order to determine the effect of base modification on the PCR, we synthesized a set of oligonucleotides containing either 8-oxodG, 8-oxodA or an abasic site, and amplified either the ICR or the full-length 90-mer using real-time PCR; primer binding sites did not span any of the modified bases (Table 1). The observation that all ICR amplification curves were equivalent indicated that input template amounts were equal and that the ICR was amplified with the same efficiency in each template (Fig. 1A). While the full-length amplification curves for the Oxo CONTROL and OxodG1 templates were superimposable, there was a substantial right-shift in the OxodA1, OxodG2T, and Abasic amplification curves (Fig. 1B). We also amplified a 90 base oligonucleotide which contained a TT dimer and a control template with normal adjacent thymidine bases (Dimer CONTROL; Table 1). A right-shift was also observed in the amplification of the full-length TT dimer template (Fig. 2B). Since the input template concentrations were held constant, this right-shifting observation indicated that the amplification efficiencies of OxodA1, Abasic,
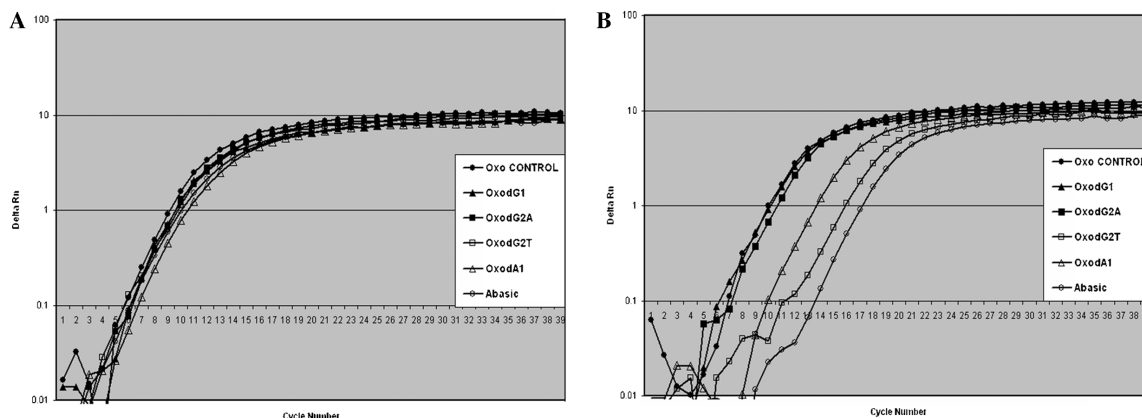
Fig. 1. Amplification of oligonucleotides containing 8-oxodG, 8-oxodA, and abasic modifications using real-time PCR. Curves represent an average of five amplifications where template concentration=1 fmole/reaction. Delta Rn is the baseline subtracted PCR product fluorescence normalized to an internal dye (ROX). (A) Amplification of 45 bp internal control region. (B) Amplification of full-length oligonucleotide (85 bp PCR product).

Fig. 2. Amplification of oligonucleotides containing *cis–syn* thymidine dimer modifications using real-time PCR. Curves represent an average of five amplifications where template concentration=1 fmole/reaction. Delta Rn is the baseline subtracted PCR product fluorescence normalized to an internal dye (ROX). (A) Amplification of 45 bp internal control region. (B) Amplification of full-length oligonucleotide (85 bp PCR product).
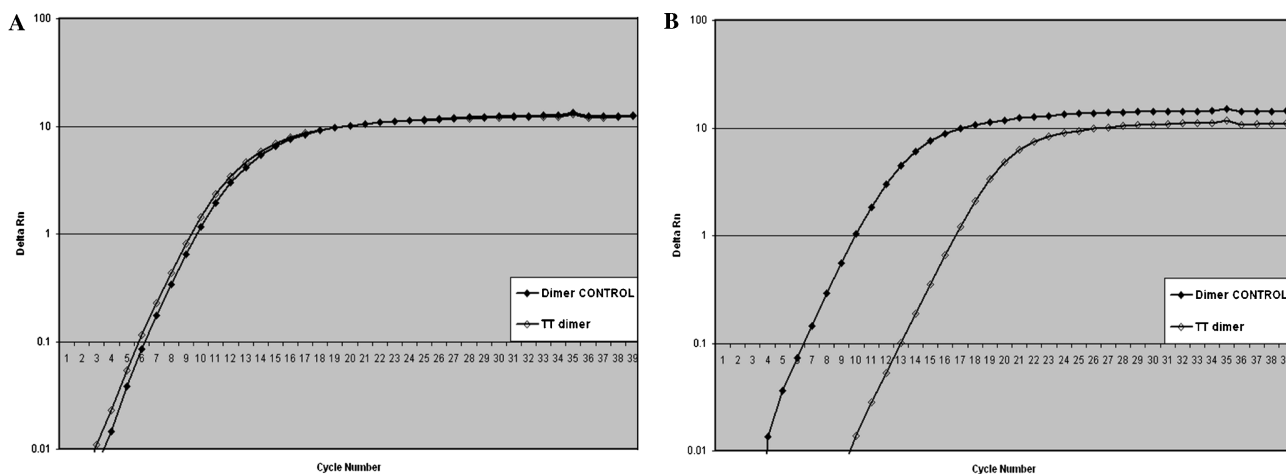
TT dimer, and OxodG2T templates were substantially reduced.

Estimation of RTC efficiency for unmodified and modified templates

We developed the RTC method to quantify differences in the amplification efficiencies of modified templates. We determined C_{TU} and C_{TM} at six template amounts (1 amole–100 fmole) for each oligonucleotide and calculated the RTC efficiencies using Eq. (8) (Tables 2 and 3). The average RTC efficiencies of the Oxo CONTROL and Dimer CONTROL templates were 0.615 and 0.795, respectively. This observation that the RTC efficiencies of the controls were less than 1.0 suggests that the inherent efficiency of the ICR was higher than that of the full-length template reaction.

While the RTC efficiency of the Oxo CONTROL and OxodG1 templates showed no statistically significant difference ($p = 0.05$), the mean RTC efficiencies of the OxodA1 and Abasic were 0.114 and 0.009 which represented decreases of 81.2% and 98.5%, respectively, when compared to the Oxo CONTROL template (significantly different at $p < 0.001$ in both cases). The mean RTC efficiency from the TT dimer template was 0.00692 which, when compared to the Dimer CONTROL template, represented a 99.1% decrease in RTC efficiency (significantly different at $p < 0.001$). These observations, taken together, suggest that different lesions on input DNA template alter amplification to differing degrees.

The position of multiple 8-oxodG modifications relative to one another influenced the PCR. While the presence of two 8-oxodG modifications separated by 13

Table 2
RTC amplification efficiencies

Input template	Mean C_{TU}[a]	Mean C_{TM}[b]	$\Delta C_{T\ (U-M)}$	RTC (E)[c]	Mean RTC (E)	SD	CV[d]
Oxo CONTROL							
100 fmole	3.78	4.20	−0.412	0.752	0.615	0.0936	0.152
10 fmole	6.84	7.33	−0.486	0.714			
1 fmole	9.95	10.8	−0.858	0.552			
100 amole	13.3	14.1	−0.842	0.558			
10 amole	16.8	17.7	−0.916	0.530			
1 amole	20.3	21.1	−0.772	0.586			
OxodG1							
100 fmole	3.34	3.49	−0.149	0.902	0.683	0.151	0.221
10 fmole	6.09	6.44	−0.348	0.786			
1 fmole	9.57	10.1	−0.557	0.680			
100 amole	12.7	13.7	−0.952	0.517			
10 amole	16.2	17.1	−0.952	0.517			
1 amole	19.8	20.3	−0.518	0.698			
OxodG2A							
100 fmole	3.38	4.04	−0.666	0.630	0.581	0.0692	0.119
10 fmole	6.25	6.86	−0.604	0.658			
1 fmole	9.51	10.6	−1.11	0.465			
100 amole	13.2	13.9	−0.733	0.602			
10 amole	16.9	17.8	−0.883	0.542			
1 amole	20.2	21.0	−0.758	0.591			
OxodG2T							
100 fmole	3.53	8.89	−5.36	0.0240	0.0150	0.00504	0.336
10 fmole	6.32	12.3	−6.00	0.0156			
1 fmole	9.74	15.9	−6.15	0.0140			
100 amole	13.2	19.4	−6.15	0.0141			
10 amole	16.6	22.9	−6.31	0.0126			
1 amole	19.2	25.9	−6.74	0.00938			
OxodA1							
100 fmole	4.80	7.65	−2.85	0.139	0.114	0.0222	0.195
10 fmole	7.30	10.2	−2.87	0.137			
1 fmole	10.5	13.6	−3.11	0.115			
100 amole	13.8	16.9	−3.11	0.116			
10 amole	17.2	20.7	−3.45	0.0914			
1 amole	20.4	24.0	−3.55	0.0850			
Abasic							
100 fmole	4.37	10.4	−6.06	0.0150	0.00896	0.00312	0.348
10 fmole	6.90	13.6	−6.70	0.00957			
1 fmole	10.0	17.1	−7.11	0.00726			
100 amole	13.5	20.6	−7.11	0.00722			
10 amole	16.8	23.9	−7.11	0.00720			
1 amole	20.2	27.2	−7.07	0.00746			

[a] Mean C_{TU} values were calculated by averaging five amplifications of the internal control region at a threshold (T) of 1.0.
[b] Mean C_{TM} values were calculated by averaging five amplifications of the full-length oligonucleotide at a threshold (T) of 1.0.
[c] RTC efficiencies were derived using Eq. (8).
[d] CV is the coefficient of variation calculated by dividing the standard deviation of the RTC by the mean RTC.

bases (OxodG2A) had no influence on RTC efficiency, the mean RTC efficiency from reactions containing templates with two adjacent 8-oxodGs (OxodG2T) was 0.0150. This represented a 97% decrease in comparison to the Oxo CONTROL (significantly different at $p = 0.001$). This suggested that the progression of *Taq* polymerase was strongly impeded by the juxtaposition of 8-oxodG bases.

Discussion

The RTC method was designed to investigate the effect of base modifications on template amplification efficiency. In early real-time PCR cycles, replication of the full-length modified oligonucleotide gave rise to unmodified PCR products which were exponentially amplified in subsequent cycles. Even though the

Table 3
RTC amplification efficiencies[a]

Input template	Mean C_{TU}	Mean C_{TM}	$\Delta C_{T\,(U-M)}$	RTC (E)	Mean RTC (E)	SD	CV
Dimer CONTROL							
100 fmole	3.58	3.70	−0.124	0.918	0.795	0.0968	0.122
10 fmole	6.14	6.37	−0.228	0.854			
1 fmole	9.69	9.92	−0.228	0.854			
100 amole	12.8	13.2	−0.374	0.772			
10 amole	16.1	16.7	−0.580	0.669			
1 amole	19.3	19.8	−0.509	0.703			
TT dimer							
100 fmole	3.46	10.2	−6.71	0.00953	0.00692	0.00134	0.194
10 fmole	6.02	13.2	−7.15	0.00702			
1 fmole	9.30	16.6	−7.33	0.00621			
100 amole	12.6	19.8	−7.22	0.00669			
10 amole	15.9	23.3	−7.35	0.00614			
1 amole	19.1	26.5	−7.40	0.00592			

[a] C_{TU}, C_{TM}, RTC, and CV were calculated as described in Table 2.

amplification curves of unmodified and some modified templates had similar exponential phases, we observed a rightward shift in the amplification curves of templates with single 8-oxodA, abasic site, TT dimer or two tandem 8-oxodG modifications. This shift stemmed from a prolonged lag phase that could be described as a difference in C_T values and translated into RTC efficiencies. Although a single 8-oxodG base had no detectable effect on RTC efficiency, the presence of a single 8-oxodA, abasic site, and TT dimer modifications dramatically reduced RTC efficiencies by 81.2%, 97.6%, and 99.1%, respectively. Two tandem 8-oxodG bases reduced RTC efficiency by 98.5%. For a given template, we observed no correlation between input template amount and RTC efficiency.

When present in synthetic templates, 8-oxodG, 8-oxodA, and abasic sites are known to retard but not absolutely block extension by the Klenow fragment of *E. coli* DNA polymerase I [3,23–26] and *Taq* DNA polymerase is able to slowly bypass *cis–syn* thymidine dimers [34]. These properties are consistent with our observation that replication of some damaged templates is impeded, but not absolutely blocked, during early rounds of the PCR.

The RTC method normalized the observed C_T value for each full-length PCR to the ICR PCR C_T value in calculating amplification efficiency. In deriving the RTC formula, we assumed that the ICR amplification efficiency was 100% because this region contained no base modifications. We calculated RTC efficiencies for unmodified templates based on simulated ICR efficiencies in the 80–100% range and found no significant effect on RTC efficiencies (data not shown). More refined mathematical models [18,21,35–40] may be needed to detect subtle differences between the amplification efficiencies of undamaged templates and templates containing modifications that have small effects on *Taq* polymerase progression.

In order to prepare an appropriate control template for the TT dimer template, we made several thymidine substitutions in the Oxo CONTROL sequence (Table 1). We note that the RTC efficiency from the Dimer CONTROL template (0.795) was greater than that of the Oxo CONTROL template (0.615; Tables 2 and 3). This difference can be explained by a reduction in the stability of secondary structure in the Dimer CONTROL template (data not shown) which resulted in improved *Taq* progression and emphasizes the need for matched controls in the RTC method.

The presence of the 8-oxo group causes pronounced changes in base stacking interactions and the phosphodeoxyribose backbone [41]. These alterations in template secondary structure could impede *Taq* DNA polymerase advancement resulting in the observed reduction in RTC efficiency. This finding, coupled with our observation that two tandem 8-oxodGs (OxodG2T) enhanced the reduction in RTC efficiency, suggests that the position of 8-oxodG modifications on a DNA template has a much greater influence in reducing template amplification than does the number of 8-oxodG modifications. The basis for QPCR methods of DNA damage detection is that the PCR is blocked by the presence of certain lesions in the DNA template which results in a decrease in amplification product [8,13–15]. These methods assume that each lesion blocks polymerase advancement to the same degree and that there are no positional effects (i.e., that two separate lesions would have the same effect as two tandem lesions). Since we found that the type and position of base damage strongly influences the RTC efficiency, some QPCR methods may underestimate or overestimate the amount of damage.

Current QPCR DNA damage assays rely on end-point analysis and incorporation of radiolabeled nucleotides in order to quantify PCR product from damaged or undamaged templates. Adaptation of real-time PCR

technology to DNA damage detection methods would allow for rate-based determination of the extent of damage and obviate the need for radiolabeled nucleotides. Our observation on the effect of base modifications on real-time amplification is an initial step in this process. Most real-time PCR protocols require a short target DNA, usually less than 150 bp to insure high amplification efficiency. However, in order to achieve detection of physiologically relevant levels of damage and estimate the sensitivity of the detection method, protocols for the real-time amplification of larger (1000–10,000 bp) targets and synthesis of long experimental templates with defined amounts of damage must be developed.

Acknowledgments

References

[1] D. Wang, D. Kreutzer, J. Essigmann, Mutagenicity and repair of oxidative DNA damage: insights from studies using defined lesions, Mutat. Res. 400 (1998) 99–115.

[2] L. Marnett, Oxyradicals and DNA damage, Carcinogenesis 21 (2000) 361–370.

[3] S.S. Wallace, Biological consequences of free radical-damaged DNA bases, Free Radic. Biol. Med. 33 (2002) 1–14.

[4] M. Cooke, M. Evans, M. Dizdaroglu, J. Lunec, Oxidative DNA damage: mechanisms, mutation, and disease, FASEB J. 17 (2003) 1195–1214.

[5] S. Loft, H. Poulsen, Cancer risk and oxidative DNA damage in man, J. Mol. Med. 74 (1996) 297–312.

[6] J. Boer, Polymorphisms in DNA repair and environmental interactions, Mutat. Res. 509 (2002) 201–210.

[7] V. Bohr, DNA damage and its processing. Relation to human disease, J. Inherit. Metab. Dis. 25 (2002) 215–222.

[8] F.M. Yakes, Y. Chen, B. Van Houten, PCR-based assays for the detection and quantitation of DNA damage and repair, in: G. Pfeifer (Ed.), Technologies for Detection of DNA Damage and Mutations, Plenum Press, New York, 1996, pp. 171–184.

[9] V. Bohr, C. Smith, D. Okumoto, P. Hanawalt, DNA repair in an active gene: removal of pyrimidine dimers from the DHFR gene of CHO cells is much more efficient than in the genome overall, Cell 40 (1985) 359–369.

[10] V. Bohr, Gene specific DNA repair, Carcinogenesis 12 (1991) 1983–1992.

[11] H. Govan, Y. Valles-Ayoub, J. Braun, Fine mapping of DNA damage and repair in specific genomic segments, Nucleic Acids Res. 18 (1990) 3823–3829.

[12] D. Kalinowski, S. Illenye, B. Van Houten, Analysis of DNA damage and repair in murine leukemia L1210 cells using a quantitative polymerase chain reaction assay, Nucleic Acids Res. 20 (1992) 3485–3494.

[13] B. Salazar, B. Van Houten, Preferential mitochondrial DNA injury caused by glucose oxidase as a steady generator of hydrogen peroxide in human fibroblasts, Mutat. Res. 384 (1997) 139–149.

[14] D. Sawyer, B. Van Houten, Repair of DNA damage in mitochondria, Mutat. Res. 434 (1999) 161–176.

[15] S. Ayala-Torres, Y. Chen, T. Svoboda, J. Rosenblatt, B. Van Houten, Analysis of gene-specific DNA damage and repair using quantitative polymerase chain reaction, Methods 22 (2000) 135–147.

[16] W. Freeman, S. Walker, K. Vrana, Quantitative RT-PCR: pitfalls and potential, Biotechniques 26 (1999) 112–125.

[17] S. Bustin, Quantification of mRNA using real-time reverse transcription PCR (RT-PCR): trends and problems, J. Mol. Endocrinol. 29 (2002) 23–29.

[18] K. Livak, ABI Prism 7700 Sequence Detection System, User Bulletin 2, PE Applied Biosystems (1997).

[19] K. Livak, T. Schmittgen, Analysis of relative gene expression data using real-time quantitative PCR and the $2^{-\Delta\Delta CT}$ method, Methods 25 (2001) 402–408.

[20] W. Liu, D. Saint, A new quantitative method of real-time reverse transcription polymerase chain reaction assay based on simulation of polymerase chain reaction kinetics, Anal. Biochem. 302 (2002) 52–59.

[21] W. Liu, D. Saint, Validation of a quantitative method for real-time PCR kinetics, Biochem. Biophys. Res. Commun. 294 (2002) 347–353.

[22] K. Asagoshi, H. Terato, Y. Ohyama, H. Ide, Effects of guanine-derived foramidopyrimidine on DNA replication, J. Biol. Chem. 277 (2002) 14589–14597.

[23] S. Shibutani, M. Takeshita, A. Grollman, Insertion of specific bases during DNA synthesis past the oxidation-damaged base 8-oxodG, Nature 349 (1991) 431–434.

[24] S. Shibutani, V. Bodepudi, F. Johnson, A. Grollman, Translesional synthesis on DNA templates containing 8-oxo-7,8-dihydrodeoxyadenosine, Biochemistry 32 (1993) 4615–4621.

[25] M. Takeshita, C. Chang, F. Johnson, S. Will, A. Grollman, Oligodeoxynucleotides containing synthetic abasic sites, J. Biol. Chem. 262 (1987) 10171–10179.

[26] S. Shibutani, M. Takeshita, A. Grollman, Translesional synthesis on DNA templates containing a single abasic site, J. Biol. Chem. 272 (1997) 13916–13922.

[27] J. Gutteridge, B. Halliwell, Free Radicals in Biology and Medicine, third ed., Oxford University Press, New York, 1999.

[28] M. Gait, DNA/RNA synthesis and labeling, Curr. Opin. Biotechnol. 2 (1991) 61–68.

[29] B. Sproat, Chemistry and applications of oligonucleotide analogues, J. Biotechnol. 41 (1995) 221–238.

[30] S. Anderson, A. Bankier, B. Barrell, M. de Bruijn, A. Coulson, J. Drouin, I. Eperon, D. Nierlich, B. Roe, et al., Sequence and organization of the human mitochondrial genome, Nature 290 (1981) 457–462.

[31] V. Bodepudi, S. Shibutani, F. Johnson, Synthesis of 2′-deoxy-7,8-dihydro-8-oxoguanosine and 2′-deoxy-7,8-dihydro-8-oxoadenosine and their incorporation into oligomeric DNA, Chem. Res. Toxicol. 5 (1992) 608–617.

[32] A. Andrus, Evaluating and isolating synthetic oligonucleotides: the complete guide, User Bulletin 13, PE Applied Biosystems, 1987.

[33] R. Rasmussen, Quantification on the LightCycler instrument, in: S. Meuer, C. Wittwer, K. Nakagawara (Eds.), Rapid Cycle Real-time PCR: Methods and Applications, Springer Press, Heidelberg, 2001, pp. 21–34.

[34] C. Smith, J. Baeten, J.S. Taylor, The ability of a variety of polymerases to synthesize past site-specific *cis–syn*, *trans–syn*-II, (6-4), and Dewar photoproducts of thymindylyl-(3′ → 5′)-thymidine, J. Biol. Chem. 273 (1998) 21933–21940.

[35] M. Pfaffl, A new mathematical model from relative quantification in real-time RT-PCR, Nucleic Acids Res. 29 (2001) 2002–2007.

[36] A. Tichopad, A. Dzidic, M. Pfaffl, Improving quantitative real-time RT-PCR reproducibility by boosting primer-linked amplification efficiency, Biotechnol. Lett. 24 (2002) 2053–2056.

[37] C. Ramakers, J. Ruijter, R. Lankanne Deprez, A. Moorman, Assumption-free analysis of quantitative real-time polymerase chain reaction (PCR) data, Neurosci. Lett. 339 (2003) 62–66.

[38] S. Peirson, J. Butler, R. Foster, Experimental validation of novel and conventional approaches to quantitative real-time PCR data analysis, Nucleic Acids Res. 31 (2003) e73.

[39] R. Rutledge, C. Cote, Mathematics of quantitative kinetic PCR and the application of standard curves, Nucleic Acids Res. 31 (2003) e93.

[40] A. Ticopad, M. Dilger, G. Schwarz, M. Pfaffl, Standardized determination of real-time PCR efficiency from a single reaction set-up, Nucleic Acids Res. 31 (2003) e122.

[41] D. Malins, N. Polissar, G. Ostrander, M. Vinson, Single 8-oxo-guanine and 8-oxo-adenine lesions induce marked changes in the backbone structure of a 25-base DNA strand, Proc. Natl. Acad. Sci. USA 97 (2000) 12442–12445.